The theory of attenuated total reflection by surface polaritons on one-sided corrugated thin films

M. Masale*

Physics Department, University of Botswana, PlBag 0022, Gaborone, Botswana

Received 25 January 2002; received in revised form 8 July 2002

Abstract

The experimental techniques of attenuated total reflection (ATR) and grating coupling were originally employed separately as probes for polaritons. The combined technique of these methods into a single probe is a very versatile tool for probing elementary surface excitations. A theoretical investigation of this single probe for surface polaritons, ATR-grating coupling, is undertaken. The emphasis is on the calculations of first-order diffuse reflectivities, which arise due to the presence of a classical grating. More specifically, the ATR set-up in the Otto configuration is considered and for ease of presentation of the results, a classical grating is thought to be deposited on only one interface of a surface-active thin-film specimen. The discussion highlights the advantages the combined technique has over either of the two methods when each is employed on its own.

PACS: 78.20.Ci

Keywords: ATR; Grating coupling; Surface polaritons

1. Introduction

Surface polaritons propagating along planar interfaces are not accessible in ordinary optical experiments whereby light of any intensity is incident on a planar specimen [1]. ATR has proved to be a powerful tool for probing surface excitations propagating along planar surfaces. Extensive experimental as well as theoretical considerations of this method may be found in the early exhaustive editions, for example, by Agranovich and Mills [2]. There have also been some investigations of surface polaritons in composite media using the ATR method [3,4]. In these investigations, the frequency-dependent dielectric function used takes into account the inhomogeneity of the surface-active medium.

The other experimental technique which has been employed with success as a probe for surface excitations is grating coupling [5,6]. Although surface roughness, of any kind, was viewed as a nuisance by perturbing the very mode under investigation [7], it was found to play a key role in potential device applications of polaritons particularly along corrugated surfaces [8]. In this regard, it was important to map out precisely the

*Corresponding author. Tel.: +267-355-2940; fax: +267-585-097.

E-mail address: masalem@mopipi.ub.bw (M. Masale).

surface profile of the media supporting the propagation of surface modes [9], which would also be essential for the evaluations of the extent to which the mode is perturbed by surface roughness [10]. Fabrication techniques for producing well-characterized gratings were soon in place [11], followed by experimental investigations of plasmon polaritons propagating on corrugated Ag films using the ATR method [12].

A classical grating, especially of small height, scatters light in a far more coherent manner than does a statistically rough surface. In view of the recent flexibility in sample preparation as well as fabrication techniques [13], grating coupling might as well be reconsidered as a probe for surface excitations. The desire to manipulate photons in a manner similar to the control of electron in solids has led to a great deal of renewed interest in a number of research areas such as, for example, localization of light and microcavity quantum electrodynamics. Indeed there have been extensive recent investigations in optical transmission of light through subwavelength hole arrays in metal films [14–16]. The arrays of periodic cylindrical cavities excite the plasmon mode in much the same way that a grating excites surface phonon polaritons in semiconductor materials. In similar studies, grating couplers in the form of an array of dots were employed in combination with a prism coupler to map out full photonic band gaps for surface plasmons in the visible window of the electromagnetic spectrum [17].

In the investigations undertaken here, grating coupling is reconsidered, but, in combination with ATR in the Otto [18] configuration. The analysis given here is closely related to the extensive experimental as well as theoretical earlier work by Schröter and Heitmann [19], using the ATR method in the Kretschmann–Raether arrangement. The combined experimental technique of ATR and grating coupling potentially has substantial advantages over either of the two constituent methods when each is employed on its own. The main results of the investigations carried out here are the first-order diffuse reflectivities. For simplicity, the treatment given is limited to isotropic thin-film specimen, with a classical grating deposited on only one of the interfaces.

2. Formalism

The ATR set-up in the Otto [18] configuration for the systems studied here is as follows: a prism of (high) dielectric constant ε_1 occupies the region $z > 0$; an air-gap, characterized by $\varepsilon_2 = 1.00$, fills the region $-d \leqslant z \leqslant 0$; the surface-active thin film, characterized by a frequency-dependent dielectric function $\varepsilon_3 = \varepsilon(\omega)$, occupies the region $-d \leqslant z \leqslant -(d + L)$; finally, a substrate of dielectric constant ε_4 fills the half-space $z \leqslant -(d + L)$. The quantities d and L are, respectively, the thicknesses of the air-gap and that of the surface-active film specimen. The single-pole frequency-dependent dielectric function is taken in the simple form [20]

$$\varepsilon(\omega) = \varepsilon(\infty) + \frac{S\omega_T^2}{\omega_T^2 - \omega^2 - \imath\Gamma\omega}, \tag{1}$$

where $\varepsilon(\infty)$ is the high-frequency dielectric constant, S measures the strength of resonance, ω_T is the TO phonon frequency and Γ is the damping parameter.

The surface profile of a classical grating, taking only the first Fourier component, is described by

$$u(x) = u_0(e^{\imath Qx} + e^{-\imath Qx}), \tag{2}$$

where u_0 is (half) the grating amplitude and $Q = 2\pi/a_0$ is the reciprocal lattice vector of a grating of period a_0. In simple systems such as those described by the dielectric function above, the polariton fields are simply plane waves and for perfectly planar surfaces these are proportional to $e^{\imath(k_{1x}x - \omega t)}$. The crystal, in a process mediated by surface roughness, imparts momentum $\pm\hbar Q$ to the incident radiation and thereby generates the diffuse fields which are proportional to $e^{\imath(k_{1x} \pm Qx - \omega t)}$. These are the first-order fields characterized by propagation in the $q_{1x}^{\pm} = k_{1x} \pm Q$ tangential components of the polariton's wave vector. In first-order perturbation theory the two types of the first-order fields couple independently to the zero-order fields. It therefore suffices to consider the first-order fields for propagation in only one of the two (q_{1x}^{-} or q_{1x}^{+}) wave numbers. In fact, reversing the sign of Q in the fields for propagation in the one wave number gives the fields for propagation in the other wave number. The nomenclature of the polariton fields adopted

here is that the amplitudes of the zero-order polariton fields are denoted by normal letters while those for the first-order fields are denoted by script letters. In p-polarization, that is, the electric field in the plane perpendicular to the interface, the polariton fields in the ℓth ($\ell = 1, 2, 3$ and 4) region are given in component form as follows:

The zero-order fields, which exist even in the absence of surface roughness, are

$$E_{\ell x} = \{A_\ell e^{-ia_\ell z} + B_\ell e^{ia_\ell z}\} e^{i(k_{1x}x - \omega t)} \tag{3}$$

and

$$E_{\ell z} = \frac{k_{1x}}{a_\ell}\{A_\ell e^{-ia_\ell z} - B_\ell e^{ia_\ell z}\} e^{i(k_{1x}x - \omega t)}, \tag{4}$$

where the perpendicular a_ℓ and tangential k_{1x} components of the polariton wave vector are, respectively, given by

$$a_\ell^2 = \pm\left(\varepsilon_\ell \frac{\omega^2}{c^2} - k_{1x}^2\right) \quad \text{and}$$

$$k_{1x}^2 = \varepsilon_1 \frac{\omega^2}{c^2}\sin^2\theta, \tag{5}$$

in which $c = 1/\sqrt{\varepsilon_0\mu_0}$ is the speed of light in vacuum. The angle of incidence of the incoming radiation, θ, must be greater than the prism-air critical angle, $\theta_c = \sin^{-1}(\sqrt{\varepsilon_2}/\sqrt{\varepsilon_1})$, if total internal reflection is to occur. The tangential component of the wave vector of the incident radiation is a conserved quantity which means that $k_{1x} = k_{\ell x}$.

The first-order fields for propagation in $q_{1x} = k_{1x} - Q$, say, are

$$\mathscr{E}_{\ell x} = \{\mathscr{A}_\ell e^{-iq_\ell z} + \mathscr{B}_\ell e^{iq_\ell z}\} e^{i(q_{1x}x - \omega t)} \tag{6}$$

and

$$\mathscr{E}_{\ell z} = \frac{q_{1x}}{q_{\ell z}}\{\mathscr{A}_\ell e^{-iq_\ell z} - \mathscr{B}_\ell e^{iq_\ell z}\} e^{i(q_{1x}x - \omega t)}, \tag{7}$$

where

$$q_{\ell z}^2 = \pm\left(\varepsilon_\ell \frac{\omega^2}{c^2} - q_{1x}^2\right). \tag{8}$$

In Eqs. (5) and (8) for the perpendicular components of the wave vectors, the upper sign (+) is taken only for fields in region one and the negative sign for fields in the other regions. The polariton fields in region one propagate freely in all spatial directions. In the other regions, however, free propagation is only parallel to the interface but the fields are attenuated, or in general modulated, in the perpendicular direction. This is to say that the fields decay away from the interface. In addition, since the fields must be bounded as $z \to -\infty$, the coefficients B_4 and $\mathscr{B}_4$ must be zero. Further, since the first-order fields originate from the corrugated surface and are therefore not part of the incident radiation, the coefficient $\mathscr{A}_1$ must be taken as zero.

2.1. The modified boundary conditions

The usual boundary conditions of electrodynamics at a planar surface now have to be modified to take into account the undulation of the surface in the z-direction. The polariton fields are referred to a coordinate system which is simply a rotation of the ordinary cartesian coordinate system through an angle γ in the x–z plane. The above mentioned rotation is in such a way that the tangential component of the electric field is always in the interface [21]. The tangential E_t and the normal E_n components of the electric field, respectively, are related to the x- and z- components according to

$$\begin{pmatrix} E_t \\ E_n \end{pmatrix} = \begin{pmatrix} \cos\gamma & \sin\gamma \\ -\sin\gamma & \cos\gamma \end{pmatrix}\begin{pmatrix} E_x \\ E_z \end{pmatrix}. \tag{9a}$$

Following Marvin et al. [22], the tangential and the normal components of the electric field may be written as follows:

$$E_t = \frac{E_x + u'(x)E_z}{\sqrt{1 + u'^2(x)}} \tag{9b}$$

and

$$E_n = \frac{E_z - u'(x)E_x}{\sqrt{1 + u'^2(x)}}, \tag{9c}$$

where $u'(x) = \partial u(x)/\partial x$. The modified boundary conditions are then continuity of E_t and εE_n at the three interfaces. In linear-perturbation theory, only the leading terms in the expansion of the exponentials in Eq. (2) for $u(x)$ are retained. The application of the modified boundary conditions leads to tedious formulas connecting the various amplitudes of the polariton fields. In these, linear combinations of the amplitudes emerge which are coefficients of $e^{i(k_{1x}x - \omega t)}$ and those of $e^{i[(k_{1x} \pm Q)x - \omega t]}$.

The coefficients of $e^{\imath(k_{1x}x-\omega t)}$ are associated with the specularly reflected intensity while those of the factor $e^{\imath(q_{1x}^{\pm}x-\omega t)}$ are associated with the diffuse reflectivities. The inadequacy of this first-order perturbation theory to account for the distribution of the different reflected intensities according to their orders should be emphasized. In first-order perturbation theory, the equations that determine the zero-order amplitudes stand alone. First-order perturbation theory therefore does not account for the deficit in the intensity of the specularly reflected beam, which is a signature of the grating. In real systems, this deficit is a consequence of the redistribution of the incident radiation among the zero- and the higher-order polariton fields. In a full theoretical treatment, the zero- and the higher-order polariton fields are only coupled if the polariton fields are expanded at least up to second-order in the grating amplitude. Retaining higher-order terms in the expansion of $u(x)$ necessitates incorporating higher-order polariton fields in the more realistic treatment of this problem. Clearly, this goes far beyond taking only the first Fourier term in the expansion of $u(x)$. An alternative realistic approach to the problem of corrugated surfaces is to employ the Chandezon method [19,23,24], which is valid even for highly modulated gratings.

3. Applications

The formalism developed in the previous section is now applied to the two systems mentioned earlier, when a grating is inscribed or deposited on only one interface of a surface-active thin-film specimen. The numerical values of the parameters used are as follows: $\varepsilon_1 = 11.70$, $\varepsilon_2 = 1.00$, $\varepsilon_4 = 1.43$, $\omega_T L/c = 1.00$ and $\omega_T d/c = 1.00$. The values of the constants in Eq. (1) for the frequency dielectric function are taken as follows [20]: $\varepsilon(\infty) = 9.09$, $S = 2.01$ and $\omega_T = 366\ \mathrm{cm}^{-1}$. The room-temperature value of the damping parameter, reduced by an order of magnitude, is $\Gamma/\omega_T = 5. \times 10^{-4}$. For this value of Γ, the corresponding experimental investigations will have to be carried out at low temperatures, where such small values of Γ are attainable. Unless otherwise stated, the grating is characterized by the amplitude and the period such that $\omega_T u_0/c = 0.05$ and $cQ/\omega_T = 0.30$, respectively.

3.1. Grating on the upper side of a thin film

The application of the modified boundary conditions at the interface $z = -d + u(x)$ leads to the following equations which connect the zero- and first-order amplitudes of the polariton fields

$$\begin{aligned} &a_2(1 - k_{1x}Q/a_2^2)u_0[A_2e^{a_2d} - B_2e^{-a_2d}] \\ &\quad - [\mathscr{A}_2e^{q_{2z}d} + \mathscr{B}_2e^{-q_{2z}d}] \\ &= a_3(1 - k_{1x}Q/a_3^2)u_0[A_3e^{a_3d} - B_3e^{-a_3d}] \\ &\quad - [\mathscr{A}_3e^{q_{3z}d} + \mathscr{B}_3e^{q_{3z}d}] \end{aligned} \tag{10a}$$

for the tangential components of the electric field, and

$$\begin{aligned} &\varepsilon_2 q_{2z}q_{3z}u_0[A_2e^{a_2d} + B_2e^{-a_2d}] \\ &\quad - \varepsilon_2 q_{3z}[\mathscr{A}_2e^{q_{2z}d} - \mathscr{B}_2e^{-q_{2z}d}] \\ &= \varepsilon_3 q_{2z}q_{3z}u_0[A_3e^{a_3d} + B_3e^{-a_3d}] \\ &\quad - \varepsilon_3 q_{2z}[\mathscr{A}_3e^{q_{3z}d} - \mathscr{B}_3e^{-q_{3z}d}] \end{aligned} \tag{10b}$$

for the normal components of the displacement vector. The uncoupled equations, that is, those in which the zero- or the first-order amplitudes stand alone are obtained from the applications of the standard boundary conditions of electromagnetism, see for example, Cottam and Tilley [1]. The diffuse reflectivity, $\mathscr{R} = |\mathscr{B}_1/A_1|^2$, is calculated from the corresponding amplitude which is

$$\frac{\mathscr{B}_1}{A_1} = \frac{N_1}{D_1}, \tag{11a}$$

where

$$\begin{aligned} N_1 = {} & 2\imath\varepsilon_1\varepsilon_2(\varepsilon_2 - \varepsilon_3)[\varepsilon_3 k_{1x}q_{1x}\eta_1 g_2 \\ & + \varepsilon_2 a_3 q_{3z}\eta_2 g_1]q_{1z}q_{2z}a_2u_0 \end{aligned} \tag{11b}$$

and

$$D_1 = [\imath\varepsilon_2 a_1\beta_2 + \varepsilon_1 a_2\beta_1][\imath\varepsilon_2 q_{1z}f_2 + \varepsilon_1 q_{2z}f_1], \tag{11c}$$

in which

$$\beta_1 = [\varepsilon_2 a_3 g_1 \cosh(a_2 d) + \varepsilon_3 a_2 g_2 \sinh(a_2 d)], \tag{11d}$$

$$\beta_2 = [\varepsilon_2 a_3 g_1 \sinh(a_2 d) + \varepsilon_3 a_2 g_2 \cosh(a_2 d)], \tag{11e}$$

$$f_1 = [\varepsilon_2 q_{3z}\eta_2 \cosh(q_{2z}d) + \varepsilon_3 q_{2z}\eta_1 \sinh(q_{2z}d)] \tag{11f}$$

$$f_2 = [\varepsilon_2 q_{3z}\eta_2 \sinh(q_{2z}d) + \varepsilon_3 q_{2z}\eta_1 \cosh(q_{2z}d)], \quad (11g)$$

$$g_1 = [\varepsilon_4 a_3 \sinh(a_3 L) + \varepsilon_3 a_4 \cosh(a_3 L)], \quad (11h)$$

$$g_2 = [\varepsilon_4 a_3 \cosh(a_3 L) + \varepsilon_3 a_4 \sinh(a_3 L)], \quad (11i)$$

$$\eta_1 = [\varepsilon_4 q_{3z} \cosh(q_{3z}L) + \varepsilon_3 q_{4z} \sinh(q_{3z}L)] \quad (11j)$$

and

$$\eta_2 = [\varepsilon_4 q_{3z} \sinh(q_{3z}L) + \varepsilon_3 q_{4z} \cosh(q_{3z}L)]. \quad (11k)$$

3.2. Grating on the underside of a thin film

Following exactly the same analysis as in the previous sub-section, the amplitude of the first-order reflected wave for propagation in $e^{\imath(q_{1x}^- x-\omega t)}$ is found to be

$$\frac{\mathscr{B}_1}{A_1} = \frac{N_2}{D_2}, \quad (12)$$

in which

$$N_2 = 2\imath\varepsilon_1\varepsilon_2^2\varepsilon_3(\varepsilon_3 - \varepsilon_4)[\varepsilon_4 k_{1x} q_{1x} + \varepsilon_3 a_4 q_{4z}] q_{1z} q_{2z} q_{3z} a_2 a_3 u_0 \quad (13)$$

and

$$D_2 = D_1. \quad (14)$$

Note that for a grating of small height, the two first-order beams emerge equi-angular about the specularly reflected beam, at the two angles ϕ^+ and ϕ^- such that

$$\phi^{\pm} = \theta \pm \Delta\theta \quad \text{with}$$

$$\Delta\theta = \tfrac{1}{2}[\tan^{-1}(q_{1x}^+/q_{1z}^+) - \tan^{-1}(q_{1x}^-/q_{1z}^-)]. \quad (15)$$

Neglecting damping ($\Gamma = 0$) and writing a_3 and q_{3z} as pure imaginary ($a_3 \to \imath|a_3|$ and $q_{3z} \to \imath|q_{3z}|$), then equating the denominator of the expression for the reflection amplitude to zero gives the polariton dispersion relation for the system under consideration.

4. Results and discussion

For purposes of illustrating the kinematics of ATR-grating coupling, the dispersion curves of surface polaritons in a thin film of thickness such that $\omega_T L/c = 1.00$ and bounded by vacuum on either side are shown in Fig. 1. The straight lines are the ATR-grating scan lines, in the frequency scan. The smooth solid line is that associated with smooth surfaces, ck_{1x}/ω_T. The other lines are for propagation in $c(k_{1x} - Q)/\omega_T$, the dashed curve, and that for propagation in $c(k_{1x} + Q)/\omega_T$, depicted as the dotted solid line. Now, since the dielectric functions across each of the interfaces differ in sign, it follows that each of the two surfaces of the thin film supports propagation of surface polaritons [1]. Consequently, there are two branches of polariton dispersion, each corresponding to one or the other surface, but nonetheless coupled through the film thickness. It is well-known that the dispersion curves for polaritons propagating along planar surfaces run far to the right of the light line in air, the discontinuous dotted line. In prism coupling, however, the prism-light line (scan line) is displaced to the right by an amount $(\sqrt{\varepsilon_1} - 1)\sin\theta$ relative the light line in air and consequently intersects the polariton curves. The points of intersection actually define the condition of the simultaneous matching of the frequency and the tangential wave vector components of the polariton and of the incoming radiation. Under these conditions, signifying the simultaneous conservation of energy and momentum, the polariton becomes radiative. The damping parameter actually broadens the cross-over point of the dispersion curve and the scan line, which for $\Gamma = 0$ is essentially a delta function. Now, recall that in first-order perturbation theory as here, the amplitudes of the zero-order fields are coupled to the amplitudes of the first-order fields only in one of the two propagation wave numbers, $q_{1x}^- = k_{1x} - Q$ or $q_{1x}^+ = k_{1x} + Q$. In terms of the kinematics of Fig. 1, therefore, these first-order reflectivities are associated with only one pair of the scan lines, either $\{k_{1x}, q_{1x}^-\}$ or $\{k_{1x}, q_{1x}^+\}$. At least in principle, the specular reflectivity (with $u_0 = 0$) is characterized by two polariton structures (dips) while each of the two first-order reflectivities possesses four polariton structures, either dips or peaks. Just like in ATR alone, dips occur when on becoming radiative the polariton removes energy from the incoming radiation. A polariton can become radiative by actually emitting radiation in which case the polariton structure

shows itself as a peak in the reflectivity spectrum [8]. The origin of this radiative character of the mode is related to the oscillatory nature of the component of the electric field E_n normal to the undulation as the surface polariton propagates along the corrugated surface. The oscillatory nature of E_n has the polariton then radiating energy more or less like an oscillating electric field dipole. In a rather simplified picture, the radiated energy is derived from the momentum $\hbar Q$ imparted to the polariton via surface roughness.

Fig. 2 shows the diffuse reflectivities in the frequency scan for the system when a grating of height $\omega_T u_0/c = 0.05$ and period $cQ/\omega_T = 0.30$ is inscribed on the upper surface of a thin film. The other relevant parameters are summarized in Section 3. Fig. 2a is the reflectivity associated with polariton propagation in q_{1x}^- and the angle of incidence is $\theta = 30°$. Fig. 2b is for propagation in q_{1x}^+ and for $\theta = 27°$. Each curve is characterized by four polariton structures, labelled ω_{iLM} or ω_{iUM} ($i = 0$ or 1), corresponding to the lower (LM) or upper (UM) branch of the polariton curves, respectively. The index subscript is used to distinguish between the polariton structures associated with the zero-order (0) and the first-order (1) scan lines. The insert, as in the following figures, is a schematic diagram of the system that is modelled. Now, for the particular parameters used here, the polariton structures corresponding to the lower mode are dips while those corresponding to the upper mode are peaks. In the case of a semi-infinite specimen, the diffuse reflectivities in ATR-grating coupling are consistently characterized by dips when the grating is on the base of the (semi-infinite) coupler prism. However, for the system when the grating is inscribed on a surface-active medium, the polariton structures are peaks [25]. The dips in the reflectivities of Fig. 2 arise possibly in part due to coupling of the modes to the incoming radiation through the thickness of the film, just like in the ATR configuration due to Kretschmann and Raether [26].

The first-order reflectivities for the system when the grating is on the underside of a thin film are shown in Fig. 3. Fig. 3a is for propagation in q_{1x}^- and the angle of incidence is $\theta = 30°$. Fig. 3b is for propagation q_{1x}^+ and the angle of incidence is

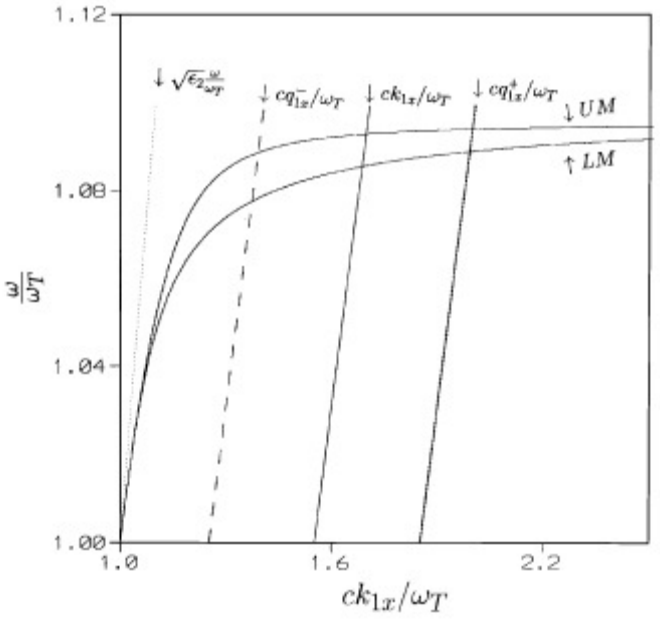

Fig. 1. Surface polariton dispersion curves in a surface-active thin film of thickness $\omega_T L/c = 1.00$ bounded by vacuum on both sides. The straight lines are the typical ATR-grating coupling frequency scan lines as follows: the solid scan line corresponds to the zero-oder reflectivity, that is, for propagation in k_{1x}. The dashed scan line corresponds to first-order propagation in $k_{1x} - Q$ and the dotted solid line is for propagation in $k_{1x} + Q$. The angle of incidence is $\theta = 27°$. The dotted line, $\sqrt{\varepsilon_2}\omega/\omega_T$, is the light line in air.

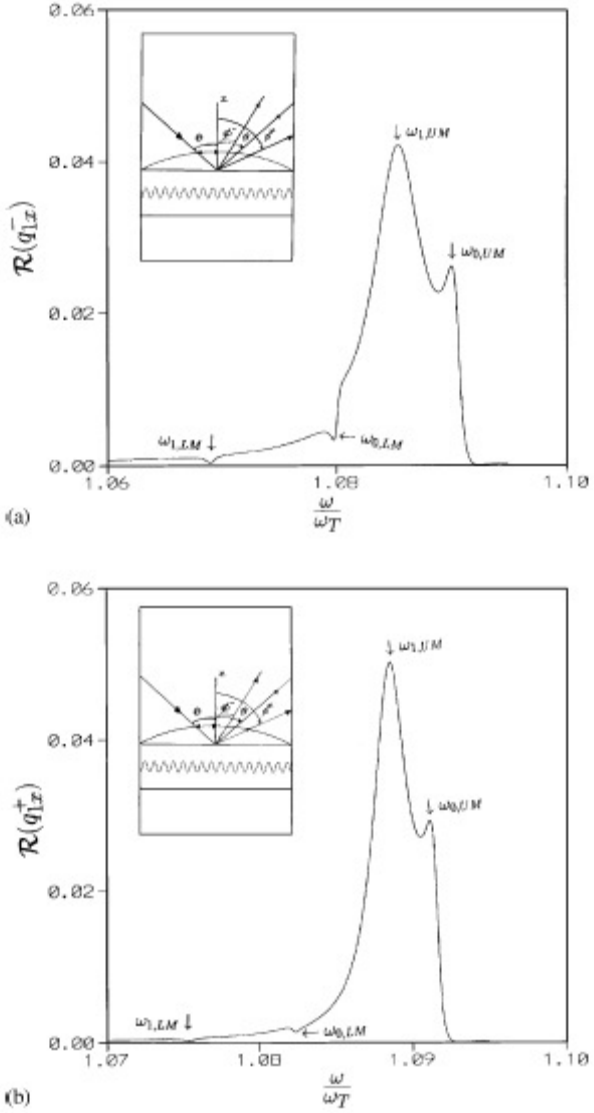

Fig. 2. (a) Diffuse reflectivities for propagation in $k_{1x} - Q$. The angle of incidence is $\theta = 30°$. A grating, characterized by the period, $cQ/\omega_T = 0.30$, and height, $\omega_T u_0/c = 0.05$, is deposited on the upper side of a surface-active thin film. The other relevant parameters, also given in the text, are: $\varepsilon_1 = 11.70$, $\varepsilon_2 = 1.00$, $\varepsilon(\infty) = 9.09$, $s = 2.01$, $\omega_T d/c = 1.00$, $\omega_T L/c = 1.00$, $\omega_T = 366.00\ \mathrm{cm}^{-1}$ and $\Gamma/\omega_T = 5.00 \times 10^{-4}$. The inset is a schematic layout of the system that is modelled. (b) Same caption as for (a) but for propagation in $k_{1x} + Q$ and $\theta = 27°$.

$\theta = 27°$. Again, the other relevant parameters, given in Section 3, are as for Fig. 2. In this case and for the parameters used all the polariton structures are peaks. It should be mentioned that,

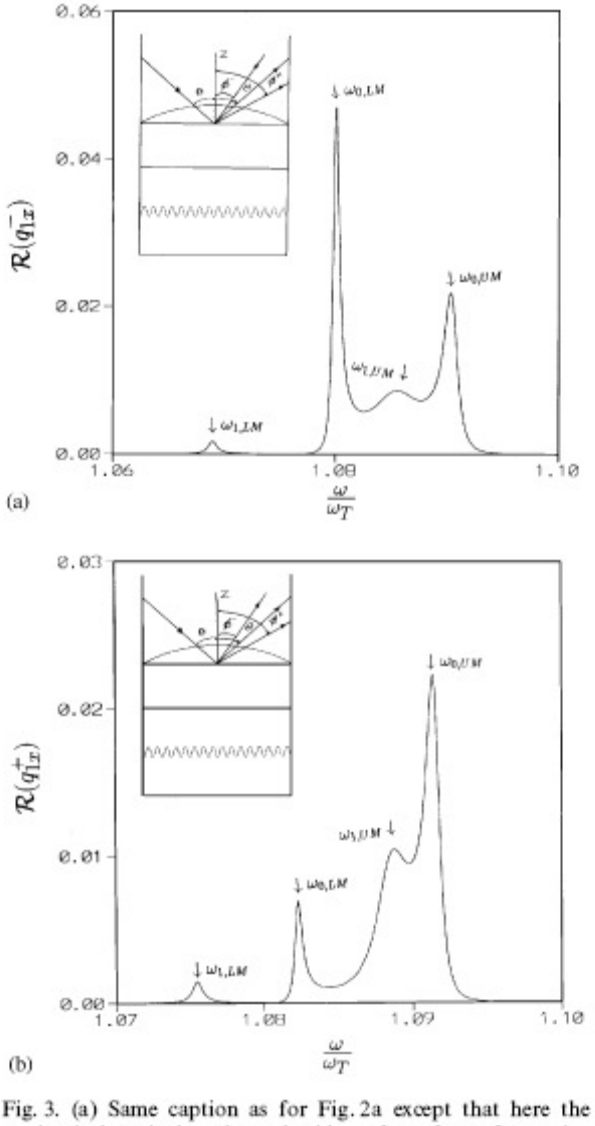

Fig. 3. (a) Same caption as for Fig. 2a except that here the grating is deposited on the underside surface of a surface-active thin-film specimen. (b) Same caption as for (a) but for propagation in $k_{1x} + Q$ and the angle of incidence $\theta = 27°$.

with surface roughness present, the radiative nature of these modes is very sensitive to all the relevant parameters, see for example, Wendler et al. [13]. Note that while the polariton structures corresponding to the two lowest modes ($\omega_{1,\mathrm{LM}}$ and $\omega_{0,\mathrm{LM}}$) of Fig. 2 are dips, the same modes manifest themselves as peaks in Fig. 3. Also, $\omega_{0,\mathrm{LM}}$ is the most radiative mode in Fig. 3a but in Fig. 3b, it is $\omega_{0,\mathrm{UM}}$ which is associated with the highest relative intensity.

It should be emphasized, however, that the first-order perturbation theory applied here is only useful in as far as predicting the frequency positions of the polariton structures in the reflectivity spectra and perhaps the radiative nature of the mode. The former prediction is, of course, taken in conjunction with the kinematical illustrations of Fig. 1. Following the earlier discussion of Section 2.1, no accurate account can be given of the actual intensities of the reflected light. Nonetheless, ATR-grating coupling is evidently the most effective and efficient method for probing surface modes compared with its constituent techniques when each one is employed on its own. To start with, in ATR alone the smallest angle of incidence is the prism-air critical angle. This means that in ATR alone the section the surface polariton dispersion curve to the left of the scan line corresponding to θ_c, namely, $ck_{1x}/\omega_T = \sqrt{\varepsilon_1}(\omega/\omega_T)\sin\theta_c$, can never be accessed. On the other hand, in grating coupling alone, the $c(k_{1x} - Q)/\omega_T$ scan lines do not intersect the branch of the surface polariton curve along the positive-axes. ATR-grating coupling is inherently associated with the largest number of effective scan lines. The effectiveness of the ATR-grating coupling scan lines is in that the higher-order reflectivities can easily be of the same order of magnitude as the specular intensity. In comparison with the higher-order reflectivities from grating coupling alone, those in ATR-grating coupling are therefore experimentally accessible. Note that in a full ATR-grating coupling theory, that is, taking as many Fourier components of $u(x)$ as necessary, at least in principle, the whole of the polariton dispersion curves can be covered for a given single angle of incidence. There is also no need to produce several gratings of different periods. The one grating of reciprocal lattice vector Q can be rotated through an angle φ about the normal to the interfaces. In that case, the surface then presents an effective reciprocal lattice vector, $Q_{\text{eff}} = Q\cos\varphi$. Again, this means that spanning the entire window of the surface polariton dispersion becomes possible even for a limited number of the lowest-order scan lines. The advantages of using first-order perturbation theory over other methods, for example, the Chandezon method, can not be over emphasized. However, there are a few points to note regarding first-order perturbation theory: analytical results for the lowest-order reflectivities are easily obtained though after tedious algebraic manipulations. These form a solid foundation for understanding the basic physics of surface modes propagating along corrugated surfaces. This is in part due to the reduction of the numerous optical parameters to which these modes are rather sensitive but nonetheless have to be incorporated in the developed algorithms. A grating of deep grooves can lead to complex phenomena such as the coversion of p- to s-polarized waves. As stated earlier, a grating of small height scatters light in a much more coherent manner than does a statistically rough surface or for that matter a highly modulated corrugated surface. Gratings of shallow grooves should therefore be of more practical interest. In these, the diffracted intensities beyond those of first-order are very weak and need not be considered. The results from first-order perturbation theory can be used to determine with ease the fundamental optical variables, for example, the value of the air-gap for optimum coupling without much computational effort. The critical optical parameters obtained this way should be useful in the preparatory stages of the corresponding experimental set-up.

5. Conclusions

The experimental technique of grating coupling as a probe for surface excitations was revisited but in combination with the method of attenuated total reflection. The Otto [18] ATR set-up was considered and, in addition, a classical grating was assumed to be deposited on only one of the interfaces of a thin film. To be more specific, the two systems considered were when the grating is inscribed either on the upper or lower interface of a surface-active thin-film specimen. Overall each system constitutes a four medium problem. The main results of these investigations were the first-order diffuse reflectivities. These were obtained within first-order perturbation theory, taking the grating as a perturbation from the otherwise assumed planar supersmooth surface. The reflectivities

are characterized by polariton structures, which are peaks or dips, depending on the radiative nature of the polariton. Dips in the reflectivity occur when the radiative mode absorbs energy from the incoming radiation. In association with the oscillatory character of the electric field normal to the undulating surface, E_n, a polariton can emit radiation. The emitted radiation then shows as a peak in the diffuse reflectivity spectrum. A case can easily be made for ATR-grating coupling being the most versatile method for probing surface modes when compared with the two constituent techniques. The combined method of ATR and grating coupling can be used to access parts of the polariton dispersion that neither of the two constituent techniques can when each is employed on its own. ATR-grating coupling is also arguably the most efficient of the three techniques by virtue of having the largest number of effective scan lines. Finally, although illustrative rather than directly predictive, the results presented here may be of value as precursors to experimental investigations. As stated earlier, the radiative nature of these modes is very sensitive to the numerous relevant parameters. Reflectivity simulations based on the analytical results derived here may therefore be useful in the selection of some specific values of the relevant parameters for optimum ATR-grating coupling.

References

[1] M.G. Cottam, D.R. Tilley, Introduction to Surface and Superlattice Excitations, Cambridge University Press, Cambridge, 1989.

[2] V.M. Agranovich, D.L. Mills, Surface Polaritons, North-Holland, Amsterdam, 1982.

[3] J.S. Nkoma, Solid State Commun. 87 (1993) 241.

[4] T. Kume, S. Hayashi, K. Yamamoto, Phys. Rev. B 55 (1997) 4774.

[5] B. Fischer, N. Marschall, H. Queisser, Phys. Rev. Lett. 27 (1971) 95.

[6] M.C. Hutley, Diffraction Gratings, Academic Press, London, 1982.

[7] A.A. Maradudin, B. Laks, D.L. Mills, Phys. Rev. B 23 (1981) 4863.

[8] H. Raether, Surface Plasmons on Smooth and Rough Surfaces and on Gratings, Springer, Berlin, 1988.

[9] V.M. Agranovich, R. Loudon, Surface Excitations, North-Holland, Amsterdam, 1984.

[10] A.A. Maradudin, A. Marvin, M. Haller, V. Celli, G. Brown, Phys. Rev. B 31 (1985) 4993.

[11] I. Pockrand, Phys. Lett. 49 A (1974) 259.

[12] D. Heitmann, H. Raether, Surf. Sci. 59 (1976) 17.

[13] L. Wendler, T. Kraft, M. Hartung, A. Berger, A. Wixforth, M. Sundram, J.H. English, A.C. Gossard, Phys. Rev. B 55 (1997) 2303.

[14] T.W. Ebbesen, H.J. Lezec, H.F. Ghaemi, T. Thio, P.A. Wolff, Nature 391 (1998) 667.

[15] L. Salomon, F. Grillot, A.V. Zayats, F. de Fornel, Phys. Rev. Lett. 86 (2001) 1110.

[16] L. Martín-Moreno, F.J. García-Vidal, H.J. Lezec, K.M. Pellerin, T. Thio, J.B. Pendry, T.W. Ebbesen, Phys. Rev. Lett. 86 (2001) 1114.

[17] S.C. Kitson, W.L. Barnes, R. Sambles, Phys. Rev. Lett. 77 (1996) 2670.

[18] A. Otto, Z. Phys. 216 (1968) 398.

[19] U. Schröter, D. Heitmann, Phys. Rev. B 60 (1999) 4992.

[20] J.S. Nkoma, D.R. Tilley, R. Loudon, J. Phys. C 7 (1974) 3547.

[21] A. Marvin, V. Celli, F. Toigo, Phys. Rev. B 11 (1975) 706.

[22] A. Marvin, V. Celli, R. Hill, F. Toigo, Phys. Rev. B 15 (1977) 5618.

[23] J. Chandezon, M.T. Dupuis, G. Cornet, D. Maystre, J. Opt. Soc. Am. 72 (1982) 839.

[24] W.L. Barnes, T.W. Preist, S.C. Kitson, R. Sambles, Phys. Rev. B 54 (1996) 6227.

[25] M. Masale, Physica B 311 (2002) 263.

[26] E. Kretschmann, H. Raether, Z. Naturforsch. 23A (1968) 2135.